

# 1–370 GHz EPR Linewidths for $K_3CrO_8$ : A Comprehensive Test for the Anderson–Weiss Model

Brant Cage,\*<sup>‡</sup> Pavle Cevc,<sup>§</sup> Robert Blinc,<sup>§</sup> Louis-Claude Brunel,<sup>†‡</sup> and Naresh S. Dalal\*<sup>‡</sup><sup>1</sup>

\*Department of Chemistry, <sup>†</sup>Department of Physics, <sup>‡</sup>Center for Interdisciplinary Magnetic Resonance, National High Magnetic Field Laboratory, Florida State University, Tallahassee, Florida 32306-4390; and <sup>§</sup>J. Stefan Institute, University of Ljubljana, Ljubljana, Slovenia

Received March 6, 1998; revised July 23, 1998

Electron paramagnetic resonance (EPR) measurements have been carried out over the frequency range of 1–370 GHz on single crystals of potassium peroxychromate ( $K_3CrO_8$ ) with the view of examining the current models of exchange narrowing of EPR signals in solids.  $K_3CrO_8$  has a simple (tetragonal) lattice structure, can be grown as single crystals pure or diluted with an isostructural diamagnetic host  $K_3NbO_8$ , and its paramagnetism can be described by a very simple ( $S = \frac{1}{2}$ ,  $I = 0$ ) spin Hamiltonian. The measurements were made at various orientations of single crystals in the Zeeman field, with emphasis on the principal directions of the  $g$ -tensor. For essentially all orientations, the linewidth decreases monotonically for measurements at resonance frequencies,  $\omega_0$ , from 1 to about 100 GHz, and then starts to increase at higher  $\omega_0$ . In order to delineate the spin exchange effects from other sources of line broadening, the measurements were repeated with a diluted spin system,  $K_3NbO_8$  containing  $\cong 0.5$  mole % of  $K_3CrO_8$ , representing the broadening effect of all the magnetic field dependent terms, such as the broadening due to the  $g$ -strain and sample holder/waveguide magnetization at the high field utilized, up to 14 T. Using these data, the  $K_3CrO_8$  linewidths were analyzed in terms of the current models of spin exchange narrowing in three-dimensional systems. A reasonably good agreement was found with the Anderson–Weiss model, when modified for various line broadening effects. The accuracy of the analysis procedure was confirmed by the comparison of the presently determined values of the exchange constant,  $J$ , and the dipolar field,  $H_p$ , with their values obtained by dc magnetic susceptibility measurements and theoretical analysis, respectively; the agreement was within 5% for  $J$  (=1.35 K) and about 25% for  $H_p$  (160 G). However, some deviations and unusual splittings were noted in measurements at 370 GHz, whose origin remains unclear. © 1998 Academic Press

## INTRODUCTION

The recent resurgence of multi-frequency electron paramagnetic resonance (EPR) spectrometers, both at the low end around 1–40 GHz (1) and at high frequencies 100 GHz and above (2, 3), has opened up a sensitive new window on the structure and dynamics of paramagnetic systems. In this re-

gard, one of the long-standing issues is the theoretical understanding of the effect of spin exchange on the shapes of EPR signals in solids. It is well established that the phenomenon of spin exchange leads to a narrowing of EPR signals, and that the exchange rates can be estimated from the variation of the signal linewidth and/or lineshape as a function of spin concentration (4). The simplest and arguably the most successful model of exchange narrowing was proposed by Anderson and Weiss (5). This model predicts that the exchange process leads to line narrowing, somewhat akin to the averaging of the dipolar and other anisotropic interactions due to motional averaging. The original Anderson–Weiss model was developed for the cases when the spin–spin exchange interaction is three-dimensional. In simple terms, the model predicts the linewidths as a function of the resonance frequency ( $\omega_0$ ), a characteristic rate of the spin exchange process, expressed as an exchange field ( $H_{ex}$ ), or an exchange frequency  $\omega_e = \gamma H_{ex}$  where  $\gamma$  is the electronic magnetogyric ratio. It predicts that when  $\omega_0$  is in the same range as  $\omega_e$ , then the magnitude of the peak to peak linewidth of the derivative mode EPR spectrum,  $\Delta H_{pp}$ , is given by  $H_p^2/H_{ex}$ , where  $H_p$  is the rigid lattice linewidth, related to the dipolar interactions in the lattice (5). Another important prediction is that  $\Delta H_{pp}$  should become largely independent of frequency  $\omega_0$  when  $\omega_0$  is significantly larger than  $\omega_e$ . This simple result, of course, changes when the exchange process becomes one-dimensional, as in the case of TMMC (6) (tetramethyl-ammonium-manganese-chloride), or two-dimensional as in the case of the layer type perovskites  $K_2MnF_4$  or  $(C_nH_{2n+1}NH_3)_2MnCl_4$  (7, 8) and the organic free radical system 3-*n*-butyl-2,4,6-triphenylverdazyl (9). In all these cases, however, the agreement with the theoretical models was only partial, and this conclusion provided the primary impetus for the present undertaking. It was thought worthwhile to carry out an in-depth evaluation of the applicability of the Anderson–Weiss model via systematic, wide-range multifrequency EPR linewidth measurements on a simple crystal lattice that is known to exhibit essentially three-dimensional exchange, and which could be described in terms of a spin Hamiltonian without the complexity of zero-field splittings and/or hyperfine interactions. While there have been many earlier attempts, to

<sup>1</sup> To whom correspondence should be addressed.

our knowledge, the earlier studies have utilized EPR probes such as  $\text{Mn}^{2+}$  (6–8, 10), or  $\text{Cu}^{2+}$  (11), or organic free radicals such as diphenylpicrylhydrazyl, DPPH (12), and triphenylverdazyl (9), which have complications due to zero-field splittings (6–8, 10) and/or hyperfine structure due to extensive delocalization (9–12). In order to obviate these complications, in the present study we have investigated  $\text{K}_3\text{CrO}_8$ . This compound was selected because (i) its EPR spectrum is a single relatively sharp peak which has been well characterized as due to a localized  $3d^1$  electron on each  $\text{Cr}^{5+}$  site (13), without the complication of any zero-field splitting or hyperfine interaction; (ii) the orbital angular momentum of the unpaired  $3d$  electron is largely quenched, so the spectrum can be well described by the Zeeman term for an  $S = \frac{1}{2}$  system; (iii) this system has been well characterized by magnetic susceptibility measurements (13), and thus offers the possibility of independent checks on the linewidth analysis procedure with more established techniques; (iv)  $\text{K}_3\text{CrO}_8$  has been proposed as a standard for the measurements of the  $g$ -value and paramagnetic spin concentration (14), but has only been characterized at 9–10 GHz.  $\text{K}_3\text{CrO}_8$  can be grown as large single crystals of the pure material, and its diluted analogs can be grown as mixed crystals using its isomorphous diamagnetic host  $\text{K}_3\text{NbO}_8$ , as described elsewhere (13).

Earlier studies (13) have established that the EPR line positions for  $\text{K}_3\text{CrO}_8$  can be well described by the following, simple effective spin Hamiltonian,

$$H = \beta g_{\parallel} H_z S_z + \beta g_{\perp} [H_x S_x + H_y S_y] \quad [1]$$

with  $g_{\parallel} = 1.9433 \pm 0.0005$  and  $g_{\perp} = 1.9854 \pm 0.0005$ . Moreover, the earlier susceptibility measurements down to 4.2 K demonstrated that the susceptibility can be well described in terms of a three-dimensional exchange constant  $J = 1.35$  K, without any complication of any ensuing structural or magnetic phase transition (13).  $\text{K}_3\text{CrO}_8$  thus appeared to be an ideal model compound to serve as a basis for testing the exchange narrowing concepts. This work presents our linewidth data over the frequency range of 1–370 GHz and discusses it in terms of the current exchange narrowing models.

## EXPERIMENTAL DETAILS

### Materials Synthesis

$\text{K}_3\text{CrO}_8$  was prepared by a minor modification of the method of Riesenfeld (15), as described earlier (13). The purity of the crystal used was checked by x-ray analysis, which agreed fully with the structure described by Stomberg and Brosset (16). The crystal belongs to the tetragonal system and the unique direction,  $c$ -axis, was easily identified as the longest dimension.

Powder of  $\text{K}_3\text{NbO}_8$  doped with  $\text{K}_3\text{CrO}_8$  in small amounts was made by the method of Balke and Smith (17). EPR measurements confirmed that the doping was successful at

about the 0.5% level, in agreement with our earlier studies (13).

### EPR Measurements

L-band (1–1.20 GHz) EPR measurements were performed at J. Stefan Institute, University of Ljubljana, Ljubljana, Slovenia, using a bridge equipped with a loop-gap resonator.

X-band (9.5 GHz) and Q-band (35.2 GHz) measurements were made using a Varian E-line spectrometer. Measurements were made by orienting single crystals in the three crystallographic planes  $ab$ ,  $bc$ , and  $ac$ . All measurements were performed at room temperature, and the microwave frequency was monitored with a Hewlett–Packard digital frequency counter model HP 5350B. The line positions were measured relative to DPPH (1,1 diphenyl-2-picrylhydrazyl) for which the  $g$ -value is known to be 2.0037 (18), and the magnetic field scans were calibrated by the DTBN (di-*t*-butylnitroxide) hyperfine splittings which are known to be 15.1 G (19).

EPR spectra in the regions of 110, 220, 330, and 370 GHz were obtained with the high-field electron magnetic resonance facility at the National High Magnetic Field Laboratory in Tallahassee. The EPR spectrometer design is similar to that described earlier by Mueller *et al.* (20) with the following modifications. The source of the millimeter wave radiation is a Gunn oscillator (AB Millimetre, Paris). This source is tunable over the 108–113 GHz range and is equipped with a set of Schottky-diode harmonic generators and filters which enable it to operate also at frequencies around 220 and 330 GHz (spectra at 375 were similarly obtained using a 93–98 GHz source operating at the fourth harmonic). The frequency was measured by an EIP580 counter, which also served as a phase lock source for the Gunn oscillator. The Zeeman field is provided by an Oxford Instruments Teslatron superconducting magnet that is capable of field sweeps from 0 to 17 T. The resonance absorption is measured at a fixed frequency by monitoring the transmitted power as a function of the applied magnetic field that is swept through the resonance in either the increasing or decreasing mode. A liquid helium-cooled hot-electron InSb bolometer from QMC (London, England) was used as the power detector. As usual for EPR, the spectra were recorded in the first derivative mode, using magnetic field modulation at audio frequencies (2–10 kHz).

### Theoretical Considerations

The main contributions to the EPR linewidth of this  $S = \frac{1}{2}$  system are thought to be the dipolar field broadening, spin exchange narrowing, inhomogeneous broadening,  $g$ -anisotropy between non-equivalent chromium sites, and lifetime broadening. We emphasize that the dimensionality of the exchange process is a very important factor in the analysis. For  $\text{K}_3\text{CrO}_8$ , however, there was relatively little angular variation in linewidths, hence the exchange is considered to be essentially three-dimensional. Our discussion here thus focuses on three-

dimensional systems. The interactions appropriate to three-dimensional exchange may be summarized as follows.

### A. Dipolar Broadening and Spin Exchange Narrowing

These two are the basic factors in determining the range of the EPR linewidths for any paramagnetic solid. While Kubo and Tomita (21) first presented a general theory of magnetic resonance lineshape, Anderson and Weiss (5) provided a simple conceptual model of spin exchange in three dimensions to which the measured linewidths can be compared with the theoretical predictions. The basic idea is that the spin–spin, magnetic dipolar interactions between the neighboring molecules lead to an overall broadening (via essentially an inverse  $r^3$  dependence) and the spin exchange processes lead to an averaging of this broadening, just as the Brownian motion leads to a narrowing of resonance peaks in fluids. Anderson and Weiss considered a lattice in which the spin exchange was three-dimensional, and they showed that for this case the EPR linewidth is related to the various parameters as (5)

$$\Delta H_{pp} = \frac{H_p^2}{H_{ex}} \left\{ 1 + \frac{5}{3} e^{-0.5(\omega_0/\omega_e)^2} + \frac{2}{3} e^{-2(\omega_0/\omega_e)^2} \right\}, \quad [2]$$

where  $\Delta H_{pp}$  is the peak-to-peak linewidth of the derivative of the absorption spectrum,  $H_p$  is the dipolar field,  $H_{ex}$  is the exchange field,  $\omega_0$  is the resonance frequency, and  $\omega_e$  is the exchange frequency given by  $\omega_e = \gamma H_{ex}$ . Assuming a cubic lattice with 8 nearest neighbors the exchange and dipolar fields are given by (13)

$$H_{ex} = 1.68 J(s(s+1))^{1/2}/g\mu_b \quad [3]$$

$$H_p^2 = (5.1)(g\mu_b/a_0^3)^2 s(s+1), \quad [4]$$

where  $s$  is the electronic spin quantum number,  $J$  is the exchange constant (as determined, for example, from magnetic susceptibility measurements),  $g$  is the electronic  $g$ -factor, and  $a_0$  is the distance to the nearest neighbor as determined from crystal structure. Using  $s = \frac{1}{2}$ ,  $g = 1.97$ ,  $J = 1.35$  K, and  $a_0 = 6.07$  Å for  $K_3CrO_8$ , we obtain  $H_p = 160$  G and  $H_{ex} = 1.48 \times 10^4$  G, as discussed previously (13).

In addition there is a small hyperfine contribution to the dipolar field from the 9.5% natural abundance of the  $^{53}Cr$  isotope which has  $I = \frac{3}{2}$ . Using the relation for the strong field approximation for the hyperfine contribution to the second moment given in A. Bencini and D. Gatteschi (22) with the parameters  $\Theta = 90^\circ$ ,  $I = \frac{3}{2}$ ,  $g_{\parallel} = 1.9433$ ,  $g_{\perp} = 1.9854$ ,  $A_{\parallel} = 40$  G,  $A_{\perp} = 12$  G (13), it is found that the hyperfine contribution to the second moment is  $3723$  G<sup>2</sup>.

### B. Inhomogeneous Broadening Due to $g$ -Strain and Instrumental Artifacts

There are two important factors that are essentially linear in the Zeeman field, and which are not affected by spin exchange processes but do add to the observed linewidth at all frequencies, and must be added to Eq. [2]. These are (a) the broadening due to the so-called  $g$ -strain (23), which results from a spread in the  $g$ -values as caused by the local differences in the lattice imperfections and thus crystal-field forces (strains), and (b) the possible broadening due to the magnetization of the sample holder itself at the very high magnetic fields (e.g., up to 14 T) employed in this study, and mentioned in a recent EPR study on DPPH (12) that used the same equipment. It is clear that both of the parameters can be lumped together as a term that is linear in  $\omega_0$ . An important part of the present study is that this term was evaluated directly through measurements employing a diluted sample, keeping the lattice and the instrumental parameters as similar as possible to the undiluted spin system (*vide infra*).

### C. Homogeneous Broadening

This term arises from the lifetime broadening due to the spin–lattice relaxation effects, and any other effects that lead to an exchange-independent broadening. We assume that this term is essentially frequency independent over the range of our interest, 1–330 GHz. This linewidth contribution will be represented by a constant, which will be referred to as the fourth term in Eq. [6].

In this term we also include the effect of the use of a truncated-Lorentzian lineshape in the original Anderson–Weiss model (5). It is recognized that this approximation leads to an underestimation of the calculated linewidth (24). Again, we will evaluate this contribution experimentally via a combined theoretical-experimental approach.

### D. Broadening Due to Site Splitting in Crystals

The crystal structure of  $K_3CrO_8$  shows that there are two in-equivalent  $CrO_8^{-3}$  ions per unit cell (16), and it should then be expected to observe two lines at most orientations. Peak resolution does not occur if the  $g$ -value splitting is small compared to the overall linewidth, or if exchange between the two sites is of a high frequency relative to the observation frequency.

However, a broadening of the overall linewidth due to the difference in  $g$ -values,  $\Delta g$ , of the magnetically in-equivalent sites can occur as a function of the square of the field, and the secular relationship in its simple form is (22)

$$\Delta H_{pp} = (\mu_b/8gJ)(\Delta g \times H)^2, \quad [5]$$

where  $J$  is the exchange energy between the sites, and  $H$  is the resonance field.

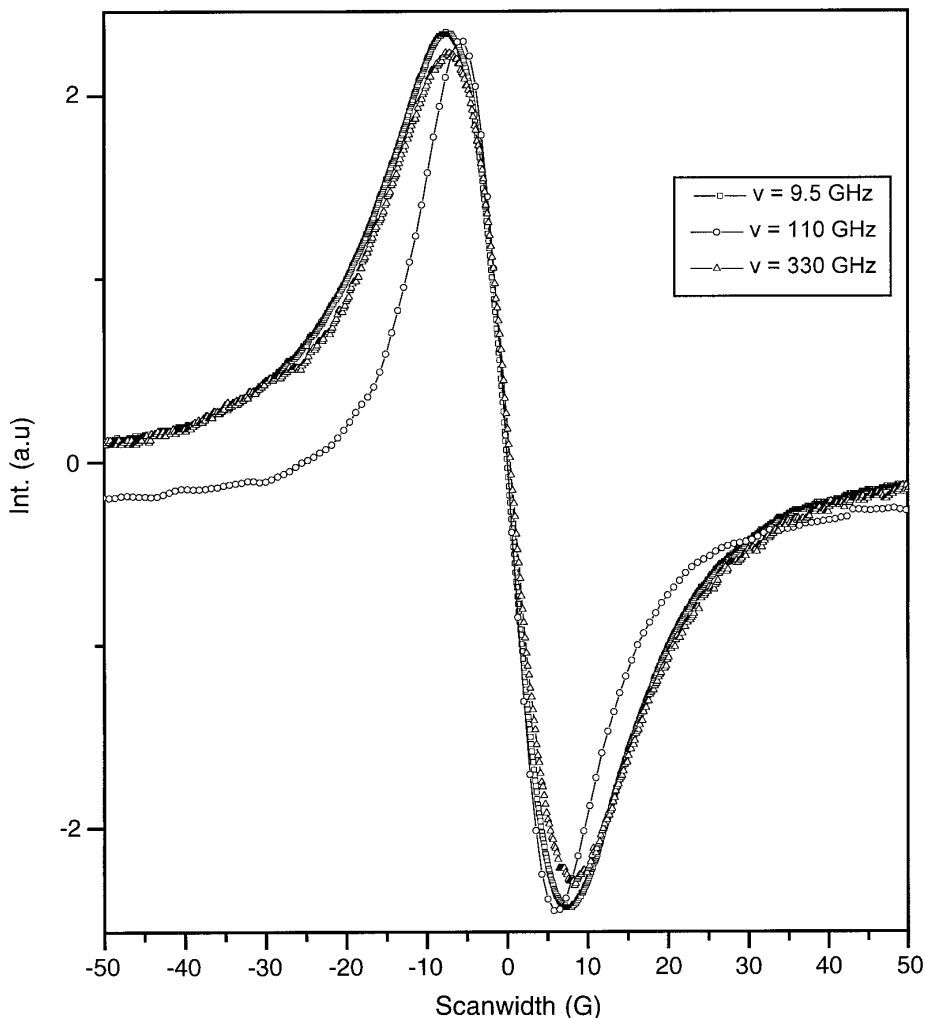


FIG. 1. Typical EPR crystal spectra of  $K_3CrO_8$  at 9.5, 110, and 330 GHz.  $H_0$  is the respective resonance field for  $H \perp c$  for each frequency.

The crystal structure of  $K_3CrO_8$  ( $I\bar{4}2d$ ) suggests that the  $\Delta g$  term in Eq. [5] is expected to be at a minimum when the highest symmetry axis, the  $c$ -axis, is perfectly parallel to the Zeeman field. For the theoretical fit of this system no attempt is made at this time to determine the exchange between non-equivalent Cr sites, and this field-dependent contribution is accounted for by an isotropic empirical square term.

#### Overall Dependence of the Linewidth on the Resonance Frequency

Based on the above discussion, the following equation represents the sum of all the contributions outlined,

$$\Delta H_{pp} = \frac{H_p^2}{H_{ex}} \left\{ 1 + \frac{5}{3} e^{-0.5(\omega\omega_0/\omega_c)^2} + \frac{2}{3} e^{-2(\omega\omega_0/\omega_c)^2} \right\} + X\omega_0 + X'\omega_0^2 + C, \quad [6]$$

where  $X\omega_0$  is derived from Fig. 3 and represents instrumental and  $g$ -strain effects,  $X'\omega_0^2$  is an empirical parameter representing the broadening from  $g$ -anisotropy, and  $C$  is a constant representing the probe's residual linewidth, determined by spin-lattice relaxation and any other lifetime processes.

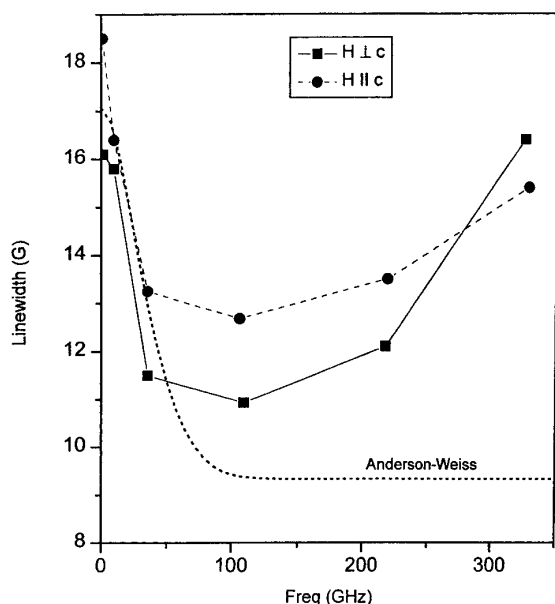
#### Experimental Results and Analysis

Figure 1 shows typical spectra from a single crystal of  $K_3CrO_8$  at three frequencies: 9.5, 110, and 330 GHz as marked. At the lower frequency side, from 1 to 35 GHz, the lineshape was found to be Lorentzian over at least 5 linewidths, in agreement with an earlier report (13). Above this range, the lines were Lorentzian in the central part, but had some deviation from the Lorentzian shape in the wings (due to magnetic-field dependent factors, *vide infra*). From a visual comparison of the peak-to-peak widths,  $\Delta H_{pp}$ , of these spectra it is clearly noticeable that  $\Delta H_{pp}$  is strongly frequency dependent: it is a

nonlinear function of frequency. This behavior is more clearly evident in Fig. 2 where  $\Delta H_{pp}$  is plotted as a function of frequency over the measured range of 1–330 GHz. It should be noted that due to the lack of sensitivity at very low frequencies, the measurement at 1 GHz was done with multiple aligned crystals. The linewidth data are presented for the two canonical orientations of the  $g$ -tensor, the  $H \parallel c$  and  $H \perp c$  directions, as marked in the figure. The dotted line is the Anderson–Weiss best fit using Eq. [2] keeping the exchange value constant, varying the dipolar term, and adding a constant homogeneous linewidth as the background width (to be discussed in more detail later). It is clear that for both orientations the low field functional dependence of  $\Delta H_{pp}$  is essentially similar with an initial relatively fast decrease followed by a shallow minimum around 100 GHz. At higher frequencies, however, the linewidth corresponding to the perpendicular feature approaches and exceeds that for the parallel orientation.

A preliminary analysis of the data in Fig. 2 indicated that while the initial decrease in the linewidths was consistent with the exchange narrowing models (*vide infra*), the mechanism causing the increase above 100 GHz was not obvious. We noted, however, that a somewhat similar broadening effect at these frequencies was also reported in a recent study of the well-known EPR standard DPPH (12) using the same instrumentation. The linear broadening detected therein was tentatively ascribed partly to instrumental artifacts (12).

It is worth noting that in the present study the cause of the broadening must be different because the effect is stronger for the  $H \perp c$  than  $H \parallel c$ , although the same probe was used in both cases. This indicated that the broadening was due perhaps to a



**FIG. 2.** Frequency dependence of  $\Delta H_{pp}$  of a single crystal of  $K_3CrO_8$  for  $H \parallel c$  and  $H \perp c$ . The dotted line is the general Anderson–Weiss best fit using Eq. [2], assuming a constant homogeneous width of 6 G.

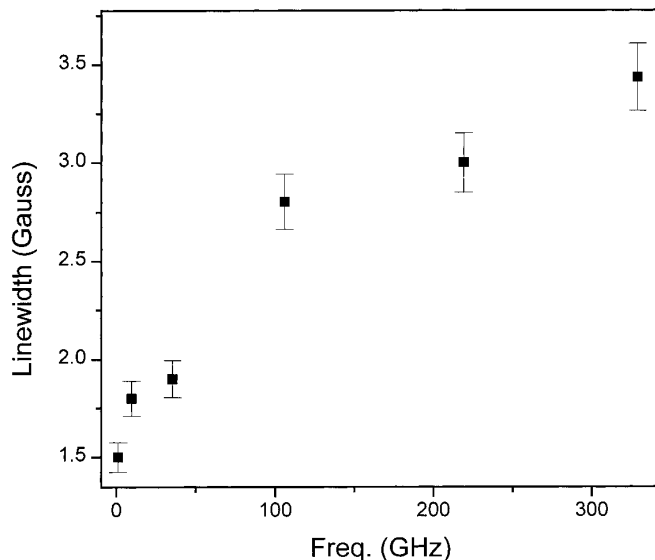


**FIG. 3.** Frequency dependence of  $\Delta H_{pp}$  for the  $\perp$  feature of the powder spectra of 0.5%  $K_3CrO_8$  diluted into a diamagnetic  $K_3NbO_8$  host.

site splitting mechanism because of the possibility of site splitting at  $H \perp c$ , but not for  $H \parallel c$ . Also, the broadening appeared to be a function of the square of the field, characteristic of site splitting, and not linear as expected for  $g$ -strain or instrumental effects.

In order to ascertain the underlying cause experimentally, and, specifically, to delineate the contributions of the actual  $K_3CrO_8$  lattice and its associated exchange effects, we carried out similar linewidth measurements on powders of 0.5 mol%  $K_3CrO_8$  substituted into its isostructural, diamagnetic host  $K_3NbO_8$ . This sample yielded spectra at essentially identical  $g$ -values as for  $K_3CrO_8$ , but with significantly (order of magnitude) narrower linewidths, in agreement with an earlier study (13) at 9.5 GHz. Figure 3 shows the frequency dependence of the linewidths for this  $K_3CrO_8$  doped  $K_3NbO_8$  lattice. We assumed that the linewidths data of Fig. 3 represent essentially all the magnetic field-dependent contributions to the linewidth of the  $CrO_8^{-3}$  probe, such as the broadening related to the  $g$ -strain effect (23), and the magnetization of the sample holder at these very high fields (12). Since the focus of the present study was to assess the effects of spin exchange on EPR linewidths, the linewidth data of Fig. 3 were thus lumped as a lattice-instrumental background effect, and were subtracted from the data in Fig. 2. The linewidth data thus corrected for the background are presented in Fig. 4 for the  $H \perp c$ .

The data of Fig. 4 were then analyzed using the Anderson–Weiss approach by a curve-fitting, iterative procedure. The overall goal was to fit the measured linewidth data to Eq. [6], which consists of four terms. The parameters in the first term (the one in parentheses) are the exchange frequency  $\omega_e$ , which is known from earlier magnetic susceptibility data (13), and the theoretical dipolar field  $H_p$  (13), both of which could also be fit to the linewidth data of Fig. 4. We note, however,  $\omega_e$  was

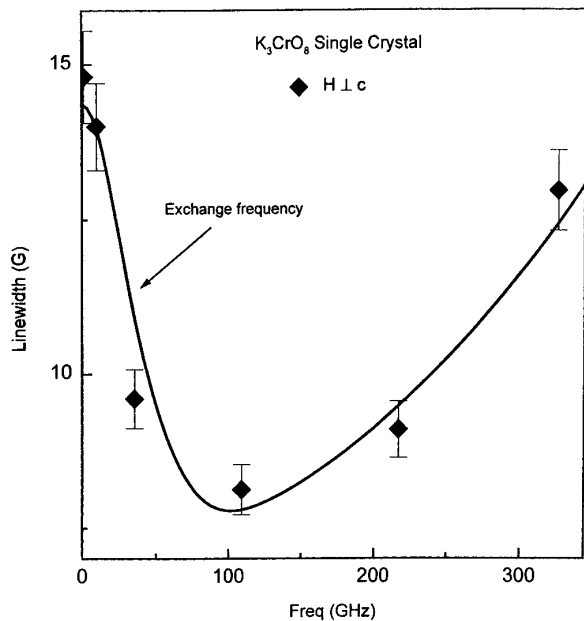


FIG. 4. Frequency dependence for  $H \perp c$  corrected for the background contributions by subtracting the data in Fig. 3 from Fig. 2.

allowed only a 5% deviation from susceptibility measurements (essentially kept constant), while the dipolar field value was allowed to vary until the best fit was attained. The contributions of the second term representing the field-dependent broadening were evaluated experimentally using a diluted sample, as discussed above, and presented in Fig. 3. The third term representing the linewidth dependence as a function of the square of the field, which is tentatively ascribed to site splitting, was also varied until a best fit was achieved. The fourth term is a constant, homogeneous background width, which is evaluated experimentally as the difference between the theoretical high field limit of  $\Delta H_{pp}$  plus the broadening terms and the experimentally observed value, which was kept constant over the entire frequency range employed in the present study. This value was measured as 4 G. In fact, since the second and fourth terms could be evaluated directly through measurements (data of Figs. 2–4) and the exchange frequency was essentially held constant, the fitting of the data required only two unknowns,  $X'$  and  $H_p$ . This methodology, in fact, enabled us to evaluate these parameters as variables, since we had only two variables and six independent observations. The solid line in Fig. 4 shows the best theoretical fit. The parameters corresponding to this best fit were

$$\omega_e = 38 \text{ GHz}$$

$$H_p = 207 \text{ G}$$

$$X' = 0.00005 \text{ s}^2 \text{ G.}$$

The above value of 38 GHz for  $\omega_e$  is within 5% of the earlier

reported value of 40 GHz (13) as derived from magnetic susceptibility data. The agreement for  $H_p$  is a bit less satisfactory; the present value of 207 G being within 25% of the earlier reported number of 160 G (which did not take into account the hyperfine field). We note, however, that the earlier value for  $H_p$  was based on a theoretical estimate; thus the value deduced here from the linewidth data is thought to be considered as a reliable number for this rather difficult to measure, but fundamentally important, parameter.

In order to add further credence to the existence of line broadening due to a site-splitting mechanism, the frequency dependence of  $\Delta H_{pp}$  for a powder sample of  $K_3CrO_8$  was measured. These are presented in Fig. 5, after subtracting the values from Fig. 3. Since symmetry related sites are not distinguished in a powder the parallel transition should have a broader linewidth throughout the entire experimental range, as was observed. The small linear broadening above 100 GHz is probably due to  $g$ -strain that is not accounted for by the dilute system in Fig. 3.

## CONCLUSIONS

To our knowledge, the present study constitutes the first comprehensive test of the effect of three-dimensional spin exchange on the widths of EPR signals that blankets the exchange frequency over such a wide range. We have utilized the same compound in single crystals, powder, and as a diluted material, which has made it possible to delineate the effect of dimensionality, as well as of broadening by processes other than spin exchange. The effect of  $g$ -strain and the possible effect of the field-induced magnetization of the sample holder were determined experimentally. The experimental data could be well fitted with the standard Anderson-Weiss model, but

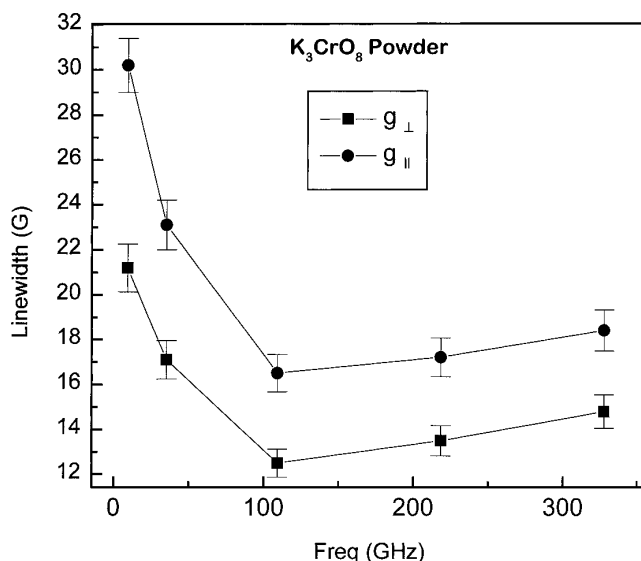
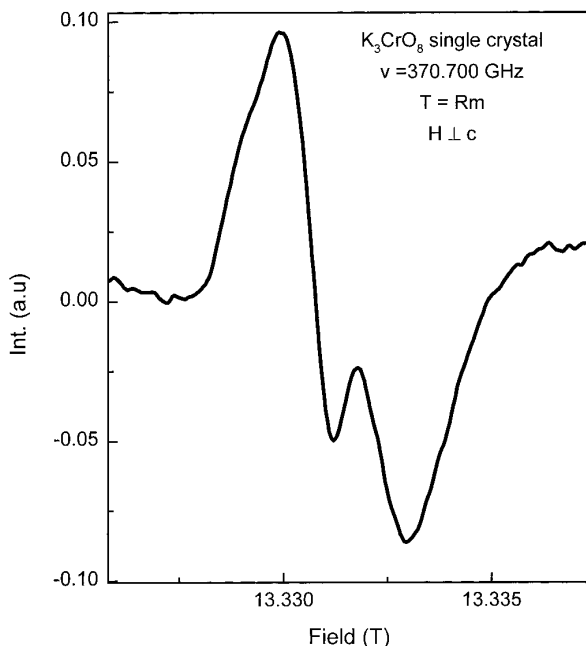


FIG. 5. The linewidth as a function of frequency of pure  $K_3CrO_8$  powder.



**FIG. 6.** A single crystal of  $K_3CrO_8$  with  $H \perp c$  at 370.700 GHz demonstrating the high field splittings, whose origin is still not clear; see text.

with appropriate corrections for the sources of broadening other than the exchange processes. The parameters obtained from the EPR data agree well with those reported earlier from magnetic susceptibility data and analysis (13). This indicates that multi-frequency EPR measurements sandwiching the exchange field could be used as a sensitive complement to the susceptibility methodology, in particular for verifying the magnitude of the dipolar field, which is not directly measurable by the latter technique.

We wish to add that the value obtained for the  $X'$  parameter implies that there exists a site-splitting effect corresponding to a  $\Delta g$  in the  $10^{-3}$  range, which seems somewhat excessive. This would indicate that in addition to site splitting there are probably other sources of broadening due to some other field-dependent cooperative phenomena present. Measurements at 370 GHz, Fig. 6, show splittings of the main peak into a doublet along with some weak sidebands. These splittings are orientation dependent, and of course field dependent, thus resembling a site-splitting effect. But it is clearly not a site-splitting effect in the usual sense, since it occurs to a lesser degree even for  $H \parallel c$ . The exact mechanism of these splittings is not yet understood, but is currently under investigation. Further measurements at 370 GHz and above could provide some clues to the mechanism underlying this effect, and in turn could serve as the basis of new theoretical models of spin

exchange effects in EPR spectroscopy. It will also be worthwhile extending this study to a case with a lower-dimensional exchange process, but still keeping the spin Hamiltonian to  $S = \frac{1}{2}$ ,  $I = 0$ .

## ACKNOWLEDGMENTS

We thank Professor Ronald Clark of the FSU Chemistry Department for his help with x-ray diffraction measurements, Dr. Luca Pardi of the NHMFL-CIMAR for helpful discussions, and the NSF for financial support.

## REFERENCES

1. J. S. Hyde and W. Froncisz, *Ann. Rev. Biophys. Bioeng.* **11**, 391 (1982).
2. L. C. Brunel, *Appl. Magn. Reson.* **11**, 417 (1996).
3. B. Cage, A. Hassan, L. Pardi, J. Krzystek, L. C. Brunel, and N. S. Dalal, *J. Magn. Reson.* **124**, 495 (1997).
4. J. A. Weil, J. R. Bolton, and J. E. Wertz, "Electron Paramagnetic Resonance," pp. 304–312, McGraw-Hill, New York (1994).
5. P. W. Anderson and P. R. Weiss, *Rev. Mod. Phys.* **25**, 1 (1953).
6. E. Siegel and A. Lagendijk, *Solid State Commun.* **32**, 561 (1979).
7. L. J. de Jongh and A. R. Miedema, *Adv. Phys.* **23**, 1 (1974).
8. H. Benner and J. P. Boucher, "Magnetic Properties of Layered Transition Metal Complexes" (L. J. de Jongh, Ed.), pp. 323–378, Kluwer Academic, Dordrecht, (1990).
9. N. S. Dalal, A. I. Smirnov, T. I. Smirnova, R. L. Belford, A. R. Katritzky, and S. A. Belyakov, *J. Phys. Chem. B* **101**, 11,249 (1997).
10. E. Pleau and G. Kokoszka, *J. Chem. Soc. Faraday Trans. II* **69**, 355 (1973).
11. D. M. S. Bagguley and J. H. E. Griffiths, *Proc. R. Soc. London A* **201**, 366 (1950).
12. J. Krzystek, A. Sienkiewicz, L. Pardi, and L. C. Brunel, *J. Magn. Reson.* **125**, 207 (1997).
13. N. S. Dalal, J. M. Millar, M. S. Jagadeesh, and M. S. Seehra, *J. Chem. Phys.* **74**, 1916 (1981).
14. N. S. Dalal, M. M. Suryan, and M. S. Seehra, *Anal. Chem.* **53**, 938 (1981).
15. E. H. Riesenfeld, *Chem. Ber.* **38**, 4068 (1905).
16. R. Stomberg and C. Brosset, *Acta Chem. Scand.* **14**, 441 (1960).
17. C. W. Balke and E. F. Smith, *J. Am. Chem. Soc.* **30**, 1637 (1908).
18. J. A. Weil, J. R. Bolton, and J. E. Wertz, "Electron Paramagnetic Resonance," p. 511, McGraw-Hill, New York (1994).
19. O. H. Griffith, D. W. Cornell, and H. M. McConnell, *J. Chem. Phys.* **43**, 2909 (1965).
20. F. Mueller, M. A. Hopkins, N. Coron, M. Grynberg, L. C. Brunel, and G. Martinez, *Rev. Sci. Instr.* **60**, 3681 (1989).
21. R. Kubo and K. Tomita, *J. Phys. Soc. Japan* **9**, 888 (1954).
22. A. Bencini and D. Gatteschi, "EPR of Exchange Coupled Systems," pp. 135–166, Springer-Verlag, New York (1990).
23. J. R. Pilbrow, "Transition Ion Electron Paramagnetic Resonance," pp. 48–51, Oxford Science Publications, (1990).
24. J. E. Gulley, D. Hone, D. J. Scalapino, and B. G. Silbernagel, *Phys. Rev. B* **1**, 1020 (1970).